Cell Reports

Report

The anti-inflammatory cytokine interleukin-37 is an inhibitor of trained immunity

Graphical abstract

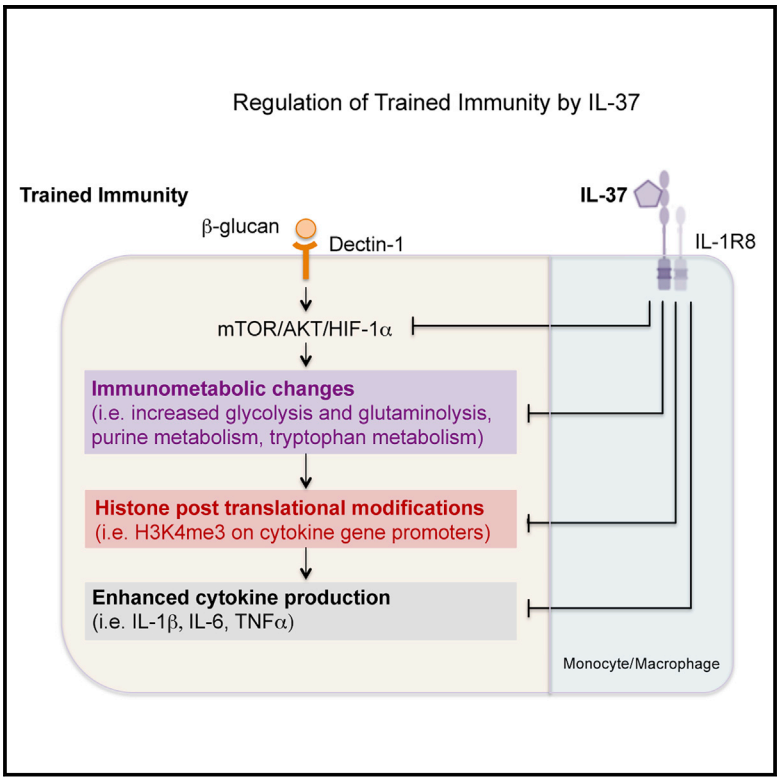

Highlights

- IL-37 counteracts the protective effects of trained immunity (TI) *in vivo*
- IL-37 suppresses pro-inflammatory cytokine production
- IL-37 reverses immunometabolic changes and histone modifications characteristic of TI

Authors

Giulio Cavalli, Isak W. Tengesdal, Mark Gresnigt, ..., Leo A.B. Joosten, Mihai G. Netea, Charles A. Dinarello

Correspondence

cdinare333@aol.com

In brief

Cavalli et al. demonstrate that the anti-inflammatory cytokine IL-37 regulates trained immunity (TI) *in vivo*. IL-37 reverses the immunometabolic changes and histone post-translational modifications underlying TI, thereby suppressing pro-inflammatory cytokine production. This regulatory role of IL-37 over myeloid-driven inflammation has implications for immune-mediated disorders and for host responses against pathogens.

Cavalli et al., 2021, Cell Reports *35*, 108955
April 6, 2021
https://doi.org/10.1016/j.celrep.2021.108955

CellPress

Cell Reports

CellPress
OPEN ACCESS

Report

The anti-inflammatory cytokine interleukin-37 is an inhibitor of trained immunity

Giulio Cavalli,[1,2,3,4,11] Isak W. Tengesdal,[1,2,11] Mark Gresnigt,[1,2,5] Travis Nemkov,[6] Rob J.W. Arts,[1] Jorge Domínguez-Andrés,[1] Raffaella Molteni,[3] Davide Stefanoni,[4] Eleonora Cantoni,[4] Laura Cassina,[3] Silvia Giugliano,[7] Kiki Schraa,[1] Taylor S. Mills,[8] Eric M. Pietras,[8] Elan Z. Eisenmensser,[6] Lorenzo Dagna,[4,9] Alessandra Boletta,[3] Angelo D'Alessandro,[6] Leo A.B. Joosten,[1] Mihai G. Netea,[1,10] and Charles A. Dinarello[1,2,12,*]

[1]Department of Medicine, Radboud University Medical Center, Nijmegen, the Netherlands
[2]Department of Medicine, University of Colorado Denver, Aurora, CO 80045, USA
[3]Division of Genetics and Cell Biology, IRCCS San Raffaele Scientific Institute, Milan, Italy
[4]Vita-Salute San Raffaele University, Milan, Italy
[5]Department of Microbial Pathogenicity Mechanisms, Leibniz Institute for Natural Product Research and Infection Biology, Hans Knöll Institute, Jena, Germany
[6]Department of Biochemistry and Molecular Genetics, University of Colorado Denver, Aurora, CO 80045, USA
[7]Laboratory of Mucosal Immunology and Microbiota, Humanitas Clinical and Research Center – IRCCS, via Manzoni 56, 20089 Rozzano (MI), Italy
[8]Division of Hematology, Department of Medicine, University of Colorado Denver, Aurora, CO 80045, USA
[9]Unit of Immunology, Rheumatology, Allergy and Rare Diseases, IRCCS San Raffaele Hospital, Milan, Italy
[10]Department of Immunology and Metabolism, Life and Medical Sciences Institute, University of Bonn, Bonn, Germany
[11]These authors contributed equally
[12]Lead contact
*Correspondence: cdinare333@aol.com
https://doi.org/10.1016/j.celrep.2021.108955

SUMMARY

Trained immunity (TI) is a *de facto* innate immune memory program induced in monocytes/macrophages by exposure to pathogens or vaccines, which evolved as protection against infections. TI is characterized by immunometabolic changes and histone post-translational modifications, which enhance production of pro-inflammatory cytokines. As aberrant activation of TI is implicated in inflammatory diseases, tight regulation is critical; however, the mechanisms responsible for this modulation remain elusive. Interleukin-37 (IL-37) is an anti-inflammatory cytokine that curbs inflammation and modulates metabolic pathways. In this study, we show that administration of recombinant IL-37 abrogates the protective effects of TI *in vivo*, as revealed by reduced host pro-inflammatory responses and survival to disseminated candidiasis. Mechanistically, IL-37 reverses the immunometabolic changes and histone post-translational modifications characteristic of TI in monocytes, thus suppressing cytokine production in response to infection. IL-37 thereby emerges as an inhibitor of TI and as a potential therapeutic target in immune-mediated pathologies.

INTRODUCTION

Immunological memory is traditionally considered a prerogative of the adaptive immune system. Conversely, the innate immune system is classically viewed as non-specific and unable to build memory. However, activated innate immune cells undergo long-term functional reprogramming, resulting in the ability to mount more robust inflammatory responses upon restimulation. Specifically, after monocytes or macrophages are exposed to certain pathogens, microbial components, or vaccines, restimulation with non-related pathogens results in enhanced production of pro-inflammatory cytokines (Netea et al., 2016, 2020a; Quintin et al., 2012). This induction of non-specific memory in innate immune cells is termed "trained immunity" (TI) (Netea et al., 2016), and it is mechanistically characterized by changes in epigenetic regulation and cell energy metabolism, sustaining enhanced production of pro-inflammatory cytokines (Arts et al., 2016a, 2016b; Cheng et al., 2014). In particular, a shift from oxidative phosphorylation to aerobic glycolysis ("Warburg effect") is essential for the induction of TI responses induced by the fungal cell wall component β-glucan (Cheng et al., 2014).

TI likely evolved in organisms without adaptive immune systems, as a mechanism to provide protection from repeated infections by inducing a state of pro-inflammatory activation. However, overly activated TI programs can induce detrimental inflammation and contribute to the development of inflammatory diseases (Bekkering et al., 2014, 2018; Mulder et al., 2019; Netea et al., 2016). It is thereby likely that tight regulatory mechanisms are in place to prevent inappropriate

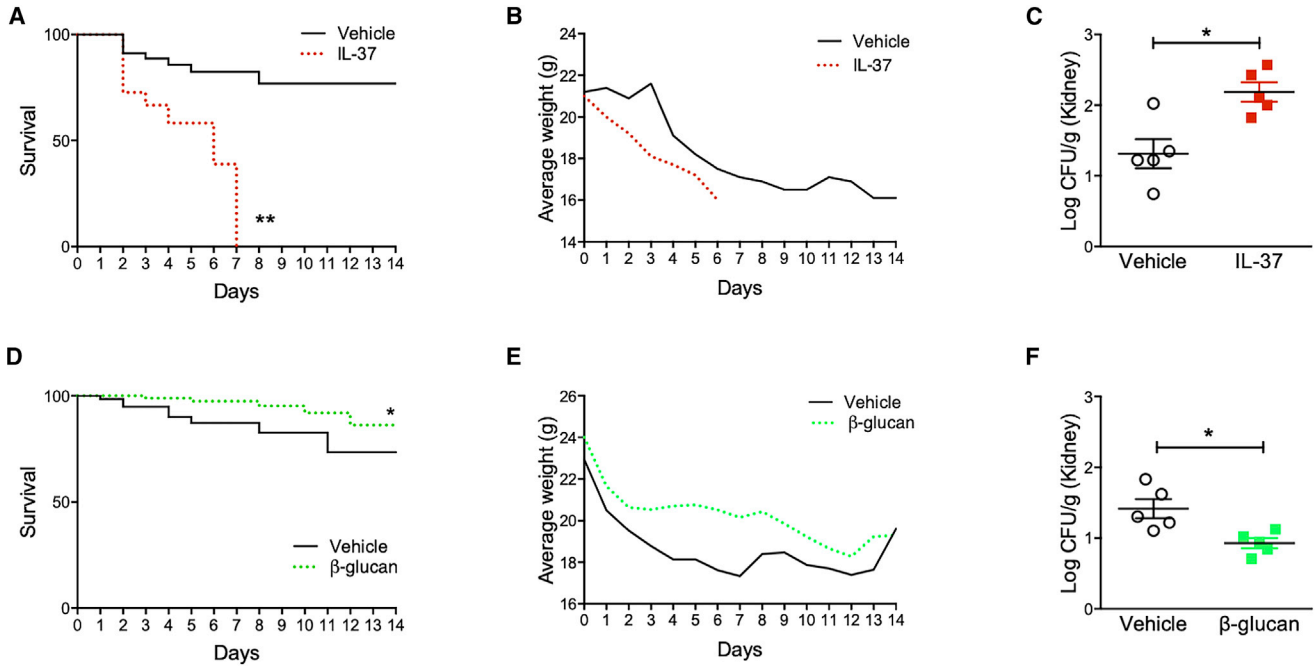

Figure 1. Effects of IL-37 and TI on the host response to *C. albicans* infection

(A) Survival rate of mice to systemic candidiasis following administration of IL-37.

(B) Weight loss.

(C) Fungal outgrowth in the kidneys.

(D) Survival rate of mice to systemic candidiasis following stimulation with β-glucan.

(E) Weight loss.

(F) Fungal outgrowth in the kidneys.

Animal survival and weight were assessed daily for 2 weeks (two experiments, product limit method of Kaplan and Meier, n = 10 mice per group). Fungal outgrowth was assessed in the kidneys 4 days after *C. albicans* infection (Mann-Whitney, n = 5 mice per group). *p < 0.05.

activation of TI. However, although several activating stimuli have been described, mechanisms suppressing TI remain largely elusive. A crucial, unanswered question pertains to the intercellular events and endogenous mediators that regulate TI.

Cytokines of the interleukin-1 (IL-1) family play a central role in innate immune responses in general, as well as TI specifically; for example, IL-1β production is enhanced in TI, while also having the capacity to induce TI *per se* (Moorlag et al., 2018). Members of the IL-1 family exhibiting anti-inflammatory properties are thereby highly promising candidates among possible regulators of TI. IL-37 is a unique IL-1 family member that curbs innate inflammation by suppressing production of cytokines (Cavalli and Dinarello, 2018; Nold et al., 2010) and confers protection against several models of inflammatory disease (Cavalli et al., 2016; Cavalli et al., 2017b; McNamee et al., 2011). In fact, the biologic effects of IL-37 extend beyond suppression of inflammatory cytokines and include complex effects on cell metabolism, such as activation of AMPK, suppression of mTOR, and increased oxidative phosphorylation, which represent a reversal of the Warburg effect (Cavalli et al., 2017a; Nold et al., 2010). Given this dual efficacy in curbing inflammation and in modulating metabolic pathways, IL-37 was a potential regulator of TI. In this study, we investigated the role of IL-37 as an inhibitor of TI.

RESULTS

IL-37 and TI have opposite effects of on host defense in a model of *Candida* infection

We first evaluated the effects of administration of recombinant IL-37 on host survival in a model of disseminated *Candida albicans* infection. We chose this model because in previous studies, transgenic mice expressing human IL-37 had increased susceptibility to *C. albicans* (van de Veerdonk et al., 2015). Experimental animals received recombinant IL-37 (0.12 mg/kg of body weight) prior to a lethal inoculum of *C. albicans* yeast (2×10^6 colony-forming units [CFU]/mouse); survival and changes in body weight were monitored daily for 2 weeks. Mice receiving IL-37 exhibited a clear reduction in survival (Figure 1A), which was mirrored by a progressive reduction in body weight, an additional indicator of health (Figure 1B). In a separate experiment, animals were sacrificed 4 days after *C. albicans* infection, and fungal burden was assessed in the kidney, a target organ for disseminated candidiasis. Mice receiving IL-37 had a markedly increased kidney fungal burden (Figure 1C).

Training with fungal cell wall β-glucan is known to induce functional reprogramming of monocytic cells, resulting in TI and protection from subsequent *C. albicans* infection (Quintin et al.,

2012). In a separate experiment, mice received a single injection of β-glucan (1 mg intraperitoneally [i.p.]) or vehicle 3 days prior to the *C. albicans* inoculum. Mice treated with β-glucan exhibited an increase in survival (Figure 1D), which was paralleled by reductions in weight loss (Figure 1E) and fungal burden in the kidneys (Figure 1F).

IL-37 abrogates the host defense and survival benefit conferred by TI

We thereafter investigated whether administration of recombinant IL-37 could revert the beneficial effects on host survival observed in mice trained with β-glucan. Mice received treatment with β-glucan and IL-37 prior to inoculum of *C. albicans* yeast. As shown in Figure 2A, upon administration of IL-37 the survival benefit conferred by TI was abrogated, and animal survival decreased to near baseline levels. Animals receiving training with β-glucan prior to infection exhibited lower fungal burden compared with vehicle-treated animals (Figure 2B); however, these protective effects were completely abrogated in mice receiving IL-37 in addition to β-glucan.

The protection against infection afforded by TI depends on increased production of pro-inflammatory cytokines by monocytes. We thus determined changes in the production of cytokines in the kidneys of experimental animals 4 days after *Candida* infection. Levels of IL-1β, IL-6, and TNF-α (Figures 2C–2E) were significantly increased in the kidneys of β-glucan-treated animals, a finding consistent with reduced kidney fungal burden and increased survival. However, in mice receiving IL-37 in addition to β-glucan, production of pro-inflammatory mediators returned to baseline levels. Of note, the inhibitory effects of IL-37 on TI were lost in mice lacking the IL-1 family receptor 8 (IL-1R8), which transduces the anti-inflammatory effects of IL-37 (Nold-Petry et al., 2015). Indeed, monocytes of trained mice lacking IL-1R8 and receiving IL-37 *in vivo* retained enhanced cytokine production upon secondary stimulation with LPS *in vitro* (Figures S1A and S1B).

As neutrophils are key players in host protection against *Candida* infection (Swamydas et al., 2016), we also determined changes in the recruitment and activation of neutrophils into the kidney of experimental animals 4 days after *Candida* infection. Levels of the neutrophil chemoattractant KC (Figure 2F), as well as the activation marker MPO (Figure 2G), were significantly increased in kidney homogenates of β-glucan-treated animals, a finding consistent with increased protection in trained mice. However, in mice also receiving IL-37 in addition to β-glucan, levels of KC and MPO returned to near baseline levels. These effects on neutrophil-related mediators were mirrored by functional differences in neutrophil recruitment: in chemotaxis assays, kidney homogenates from animals treated with β-glucan attracted significantly more neutrophils compared with controls (migration assay, Figure 2H). Again, these effects were abrogated in mice receiving IL-37 in addition to β-glucan training. Histology studies confirmed these findings (Figure 2I).

IL-37 reverses glycolysis and epigenetic changes induced by TI

Pro-inflammatory activation of monocytes in TI is sustained by metabolic reprogramming, as exemplified by increased glycolysis, accumulation of fumarate and glutamine utilization, and mevalonate accumulation in the cholesterol synthesis pathway (Arts et al., 2016a; Bekkering et al., 2018). We therefore evaluated whether abrogation of the protective effects of TI upon treatment with IL-37 was associated with metabolic changes in monocytes. Mice received IL-37 and β-glucan *in vivo*, and bone marrow-derived monocytes were subjected to metabolic analyses.

Partial-least-squares discriminant analysis (PLS-DA) indicated that TI with β-glucan and IL-37 has differential effects on the metabolic landscape of monocytes (Figure 3A), consistent with previous evidence of differential activation of mTOR and AMPK, two critical enzymes regulating metabolic reprogramming (Cavalli et al., 2017a; Cheng et al., 2014). Pathway analysis revealed that the main differentially modulated pathways of monocytes during TI induced by β-glucan or upon concomitant treatment with IL-37 included purine metabolism, the glutamine/glutamate pathway, and tryptophan metabolism (Figure 3B).

As expected, TI was associated with increased glycolysis, as demonstrated by accumulation of phosphoglycerate, phosphoenolpyruvate, and lactate; however, treatment with IL-37 restored these metabolites to baseline levels (Figure 3C). Similar changes were observed in pentose phosphate pathway intermediates and taken together, these findings are consistent with an inhibition of glycolysis (Figure 3C). To confirm these findings, bone marrow-derived monocytes stimulated with β-glucan or also treated with IL-37 were evaluated using the Extracellular Flux Analyzer (Seahorse) to determine changes in the extracellular acidification rate (ECAR), which is a proxy for glycolytic activity. Training with β-glucan resulted in increased ECAR, whereas concomitant treatment with IL-37 reduced glycolysis and glycolytic capacity (Figures 3D and 3E); training with β-glucan also increased basal oxygen consumption rate, as previously reported (Cheng et al., 2014), and this was also reverted by IL-37 (Figure S2). Furthermore, treatment with IL-37 reduced expression of genes encoding glycolytic enzymes, hexokinase (*HK1*), and phosphofructokinase (*PK*) (Figure 3F). In TI induced by β-glucan, increased glycolysis depends on activation of the AKT/mTOR/HIF-1α signaling axis (Cheng et al., 2014). Treatment with IL-37 reduced the expression of HIF-1α, consistent with previous studies indicating that IL-37 activates AMPK and suppresses mTOR (Figure 3G) (Ballak et al., 2014, 2018; Cavalli and Dinarello, 2018; Cavalli et al., 2017a; Nold et al., 2010).

In TI, metabolites generated by immunometabolic changes activate chromatin-modifying enzymes, leading to gene-specific chromatin modifications associated with enhanced transcription of genes encoding inflammatory cytokines (Netea et al., 2020a). A key epigenetic mark characterizing TI induced by β-glucan is the consolidation of histone 3 lysine 4 trimethylation (H3K4me3) at promoters of genes encoding cytokines (Netea et al., 2020a). As shown in Figure 3H, monocytes of mice trained with β-glucan showed an increase of H3Kme4 at the promoters of *TNFα* and *IL6*, which was reduced upon treatment with IL-37.

IL-37 reverses immunometabolic changes characteristic of TI

Inhibition of glycolysis by IL-37 was paralleled by the reversal of other metabolic changes characteristic of TI (Arts et al., 2016a).

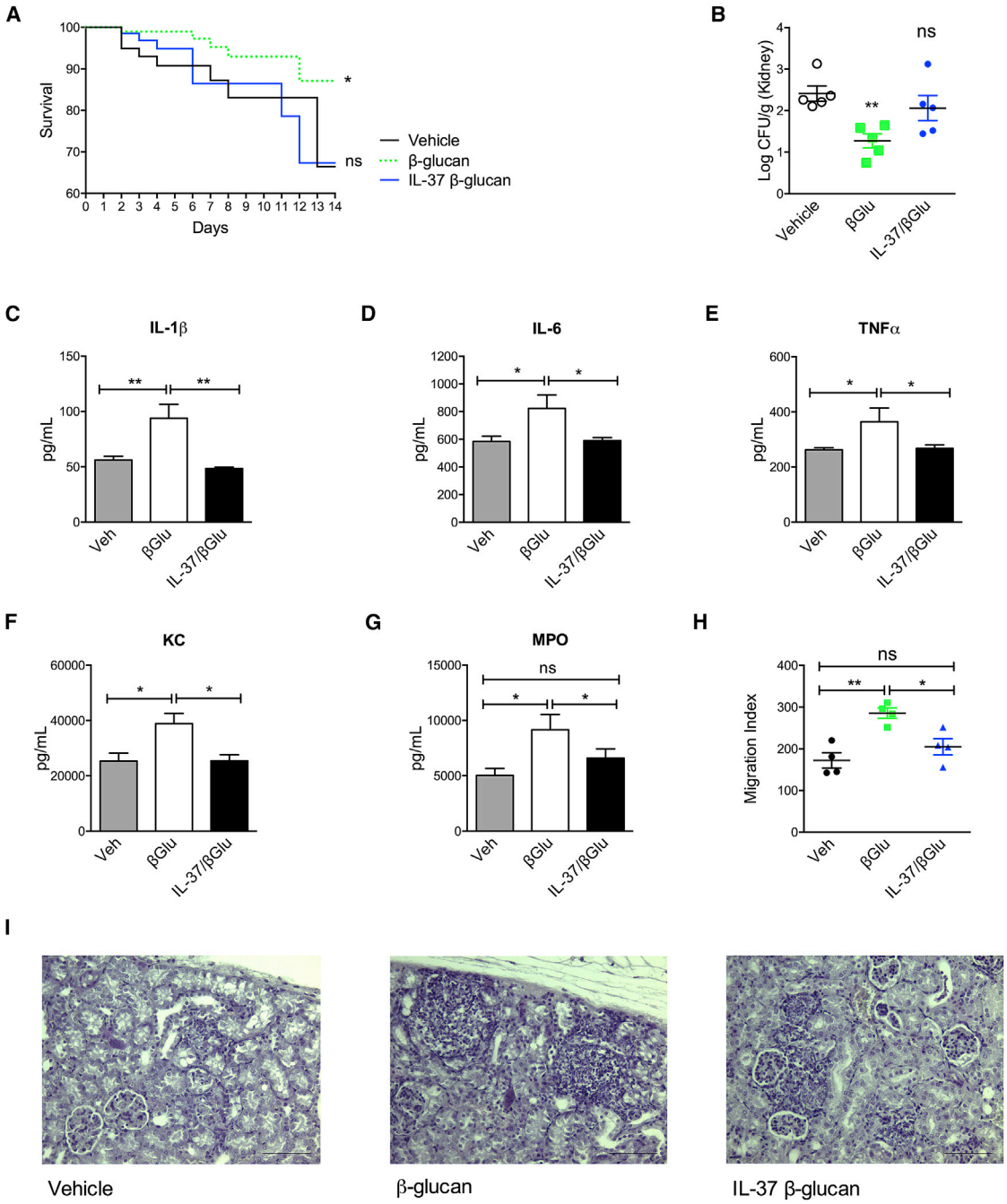

Figure 2. IL-37 suppresses TI and neutrophil responses

(A) Survival rate of mice to systemic candidiasis following administration of IL-37 and β-glucan. Animal survival was assessed daily for 2 weeks (two experiments, product limit method of Kaplan and Meier, n = 10 mice per group).

(B–G) In a separate experiment, mice were sacrificed 4 days after *C. albicans* infection: fungal outgrowth (B); levels of IL-1β (C), IL-6 (D), and TNF-α (E); and levels of KC (F) and MPO (G) were assessed in the kidneys (two experiments, ANOVA, n = 5 mice per group).

(H) Neutrophil chemotaxis was evaluated using a Bowen chamber assay: migration index: ratio of cells in lower to top chamber (one experiment, ANOVA, n = 4 mice per group).

(I) Histopathologic findings with H&E stain, original magnification 200×; scale bar, 200 μm.

ns, non-significant; *p < 0.05, **p < 0.01, and ***p < 0.005.

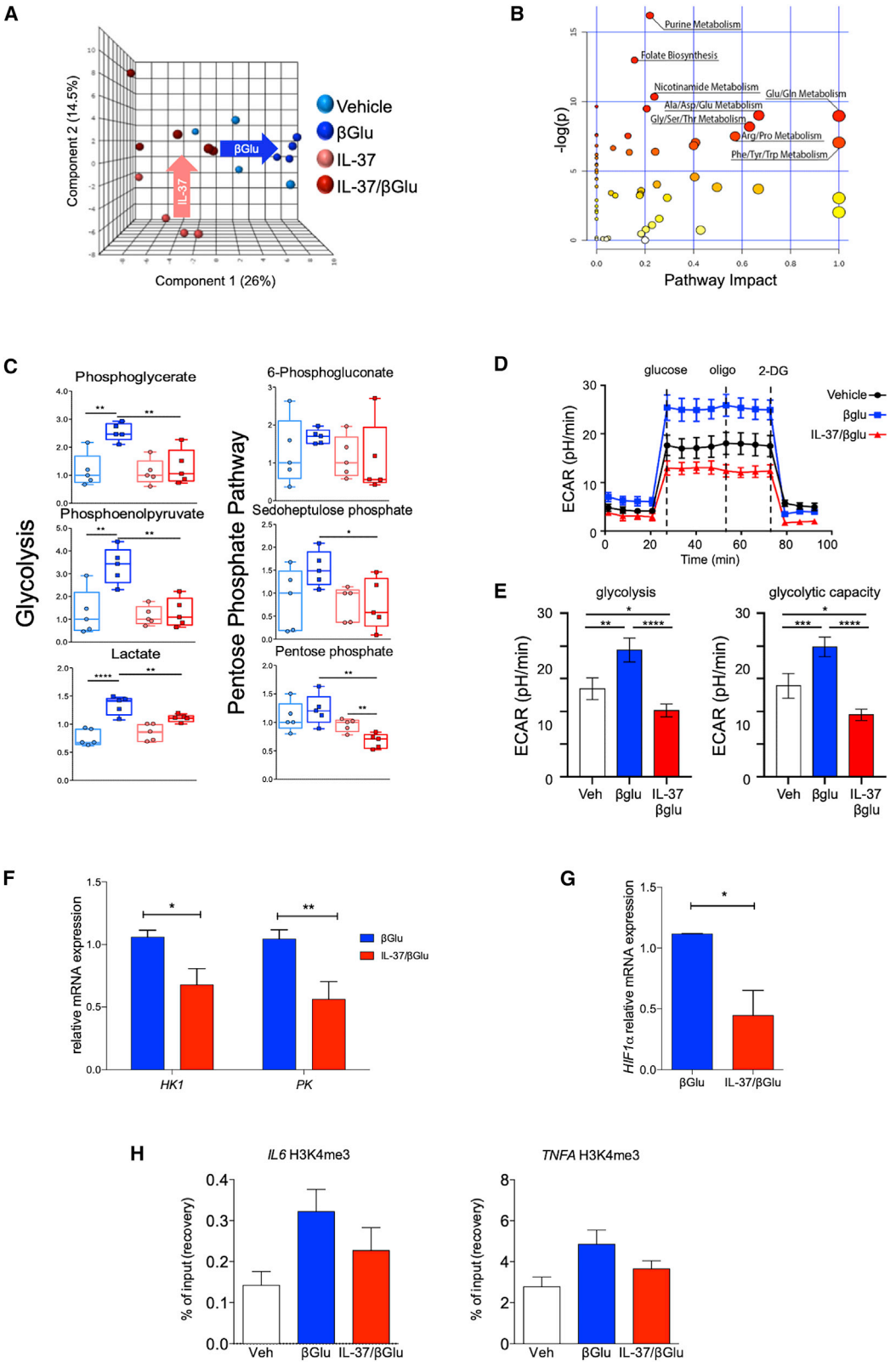

(legend on next page)

Increased glutamine metabolism through the tricarboxylic acid (TCA) cycle is a feature of trained monocytes. In this study, in the absence of isotope tracing analysis, steady-state metabolite levels indicated an increase in glutamate to fuel the TCA cycle via transamination to α-ketoglutarate; conversely, glutamate levels remained unchanged and glutamine accumulated upon IL-37 treatment (Figure 4A). Further effects of TI on the TCA cycle included accumulation of fumarate and malate. These metabolites stabilize HIF-1α (Arts et al., 2016a; Koivunen et al., 2007; Tannahill et al., 2013) and promote the epigenetic changes underlying TI (Arts et al., 2016a; Lu et al., 2012). Fumarate and malate were significantly reduced in IL-37-treated mice.

Increased glutamate fuels glutathione synthesis, which is essential to reduce oxidative stress in activated cells, such as trained monocytes. Glutathione levels were increased in monocytes from β-glucan-trained mice but were significantly lowered by treatment with IL-37 (Figure 4A). Increases in cystine, the dimerized form of rate-limiting precursor cysteine, are consistent with decreased consumption for glutathione production, as was observed upon treatment with IL-37 (Figure 4A). Higher reduced glutathione pools in trained monocytes could also be maintained by upregulation of the pentose phosphate pathway to generate NADPH (Figure 3C), which is then used as a cofactor to regenerate glutathione pools. Interestingly, monocytes of mice trained with β-glucan also exhibited increased reactive oxygen species (ROS) production compared with control, whereas treatment with IL-37 significantly reduced ROS production (Figure S3).

Purine metabolism is upregulated in TI, mainly as a result of increased glycolysis (Arts et al., 2016a, 2016b). IL-37 inhibited purine metabolism and suppressed protein glycosylation precursors UDP, UDP-glucose, and UDP-GlcNac (Figure 4B). Of note, these mediators are also required as substrates for monocyte differentiation into macrophages (Jha et al., 2015). Thus, suppression of UDP, UDP-glucose, and UDP-GlucNac by IL-37 may alter the natural development of myeloid responses following infection.

Changes in tryptophan metabolism are observed in TI as well as other inflammatory states (Arts et al., 2016a, 2016b), as a result of the activation of IDO1 (Wirthgen and Hoeflich, 2015). As shown in Figure 4C, tryptophan levels were not significantly altered by β-glucan or IL-37 treatment; however, tryptophan metabolites 8-methoxykynurenate, ɣ-oxalocrotonate, and nicotinamide were significantly increased in trained monocytes, whereas treatment with IL-37 significantly reduced these metabolites, thus indicating that IL-37 may suppress tryptophan-associated pathways in monocytes (Colabroy and Begley, 2005; Jung et al., 2009).

DISCUSSION

This study shows that the anti-inflammatory cytokine IL-37 is a regulator of TI, a pro-inflammatory cell program elicited in monocytes by exposure to pathogens, which is critically involved in host immune responses. Specifically, IL-37 functions as an inhibitor of TI, with relevant consequences on host immunity against infection.

TI is a pro-inflammatory program of monocytes and macrophages, which evolved to provide protection against infections. Although recognition of several pathogens can induce TI, induction by the *C. albicans* cell wall component β-glucan is best characterized (Netea et al., 2020a; Quintin et al., 2012). β-glucan is recognized by the monocyte receptor Dectin-1, which activates the AKT/mTOR/HIF-1α signaling axis and induces changes in cell energy metabolism, such as increased glycolysis and increased glutaminolysis through the TCA cycle (Arts et al., 2016a, 2016b; Bekkering et al., 2018; Cheng et al., 2014). Metabolic intermediates generated in these processes modulate the activity of enzymes involved in remodeling the epigenetic landscape of monocytes, leading to key epigenetic changes (i.e., H3K4me3) at promoters of genes encoding cytokines at promoters of genes encoding cytokines (Netea et al., 2020a). Thus, activation of TI programs in monocytes enhances transcription of pro-inflammatory genes, while also providing the energy that is needed for sustained inflammatory activation. Functionally, this results in hyper-responsiveness to inflammatory triggers and enhanced cytokine production (Netea et al., 2020a).

In this study, all these mechanisms were prevented by administration of IL-37. Specifically, effects of IL-37 on monocytes included suppression of HIF-1α, of glycolysis, of glutaminolysis, of epigenetic changes (H3K4me3) on genes encoding cytokines, and of enhanced cytokine production in response to infection, which are the mechanistic and functional hallmarks of TI. Of note, functional consequences of reduced cytokine production by monocytes also affected recruitment and activation of neutrophils, thus resulting in a broad suppression of the host innate immune response.

Figure 3. IL-37 inhibits glycolysis and epigenetic changes of TI

Mice were treated with β-glucan and IL-37 *in vivo*, and monocytes were obtained from the bone marrow and subjected to metabolic studies.

(A) Partial-least-squares discriminant analysis (PLS-DA) showing differential effects of TI and IL-37 on the metabolic landscape of monocytes.

(B) Pathway analysis showing the main differentially modulated pathways of monocytes during TI or upon concomitant treatment with IL-37.

(C) Changes and major modulated precursors in glycolysis and pentose phosphate pathways; y axis indicates relative abundance. In (A)–(C), one experiment, n = 5 mice per group; *p < 0.05, **p < 0.01, and ***p < 0.005; significance not shown whenever not reached.

(D) Analysis of ECAR measurements on bone marrow-derived monocytes of mice stimulated *in vitro* with vehicle (Veh), β-glucan (βglu), or β-glucan in combination with IL-37 treatment (IL-37/βglu), in basal conditions and after sequential addition of glucose, oligomycin, and 2-DG (representative experiment, n = 3).

(E) Glycolysis and glycolytic capacity of monocytes described in (D) (representative experiment, n = 3, unpaired t test; *p < 0.05, **p < 0.01, ***p < 0.001, and ****p < 0.0001).

(F) Gene expression of hexokinase (*HK1*) and phosphofructokinase (*PK*) as determined using qPCR in monocytes from mice receiving β-glucan and IL-37 *in vivo* (two experiments, n = 3, unpaired t test; *p < 0.05 and **p < 0.01).

(G) Gene expression of *HIF1a* in monocytes as described in (F) (two experiments, n = 3, unpaired t test; *p < 0.05).

(H) Monocytes were obtained as described in (A)–(C), and chromatin immunoprecipitation (ChIP) against H3K4me3 was performed in which enrichment on the IL-6 or TNF-α promoter was analyzed using qPCR (two experiments, n = 3).

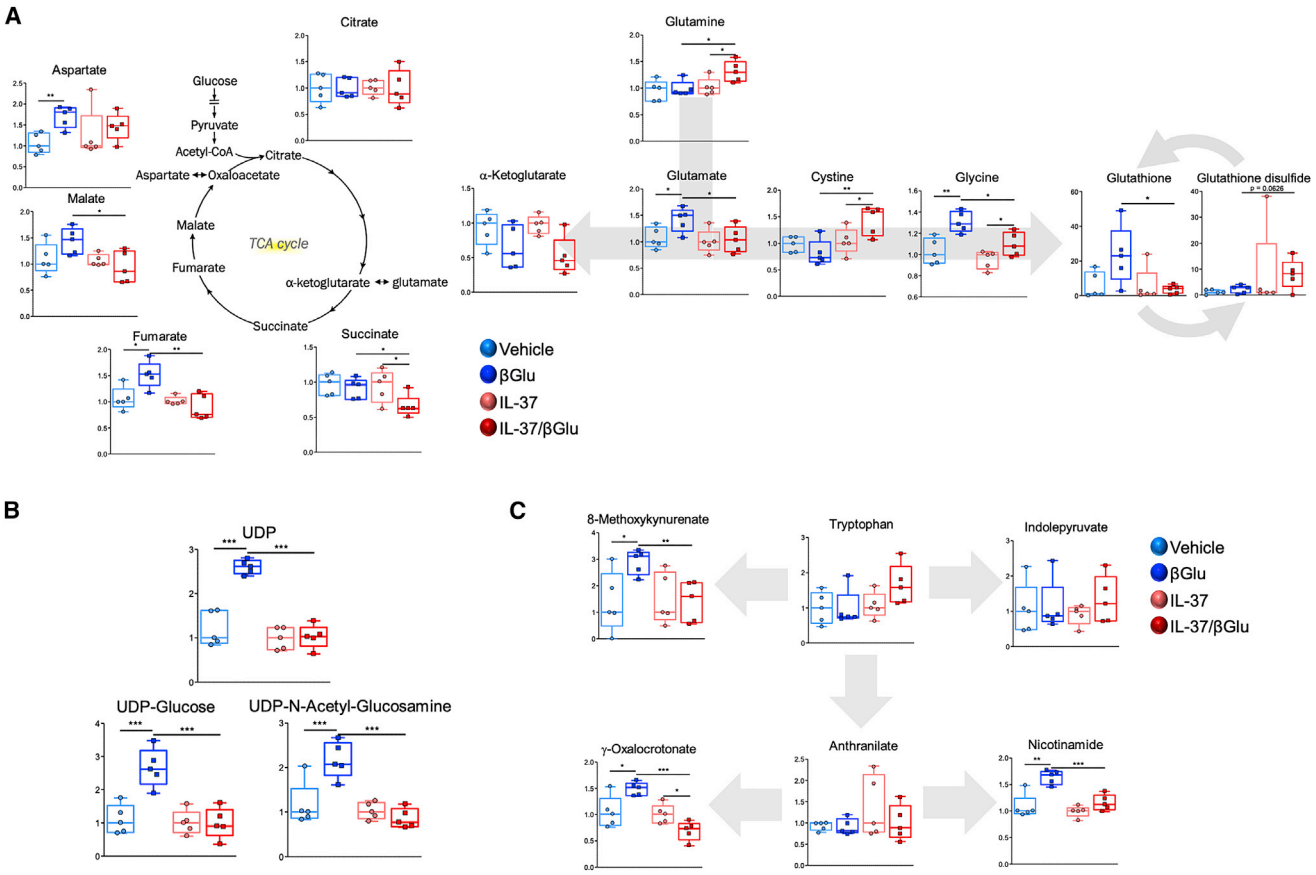

Figure 4. IL-37 reverses the metabolic changes characteristic of TI

Mice were treated with β-glucan and IL-37 *in vivo*, and monocytes were obtained from the bone marrow and subjected to metabolic studies.

(A) Changes and major modulated precursors in the TCA cycle.

(B) Changes in protein glycosylation precursors.

(C) Major modulated metabolites in tryptophan metabolism.

The y axis in (A)–(C) indicates relative abundance. One experiment, n = 5 mice per group; *$p < 0.05$, **$p < 0.01$, and ***$p < 0.005$; significance not shown whenever not reached.

The IL-1 family of cytokines is involved in TI responses (Moorlag et al., 2018). For example, administration of recombinant IL-1β enhances survival in mice subjected to inoculum of different pathogens (Czuprynski and Brown, 1987; Pecyk et al., 1989; van der Meer et al., 1988). In addition, studies of TI induced by BCG vaccination in humans demonstrated that enhanced production of IL-1β correlates with the beneficial effects of vaccination (Arts et al., 2018), whereas *in vitro* training of human monocytes is induced by IL-1β itself through epigenetic reprogramming of cells (Kleinnijenhuis et al., 2014).

IL-37 is a member of the IL-1 family of cytokines that functions as a natural suppressor of innate inflammation (Cavalli and Dinarello, 2018; Nold et al., 2010) and was thereby a highly plausible candidate among possible regulators of TI. Of note, there is no homolog gene for human IL-37 in the mouse, and it was thus not possible to directly measure IL-37 in response to TI or to conduct this study using genetically deficient animals (Cavalli and Dinarello, 2018; Nold et al., 2010); however, exogenous administration of human IL-37 to wild-type mice revealed inhibitory effects on TI. In previous studies from our group, the anti-inflammatory effects of IL-37 prevented excessive and detrimental immune responses in septic shock, endotoxemia, arthritis, and other inflammatory conditions (Ballak et al., 2014, 2018; Cavalli et al., 2016, 2017a; McNamee et al., 2011; Nold et al., 2010). Here, we show that IL-37 also inhibits TI, an appropriate immune mechanism that boosts host immunity against infection. Thus, the net effects of IL-37 on immunity are context dependent: suppression of excessive inflammation is beneficial, whereas suppression of appropriate immune responses can be detrimental.

IL-37 exerts anti-inflammatory effects through different mechanisms of action: intracellular IL-37 translocates to the nucleus, where it suppresses transcription of pro-inflammatory genes (Bulau et al., 2014; Li et al., 2019; Ross et al., 2013); extracellular IL-37 binds the IL-18 receptor α (IL-18Rα) and recruits the IL-1 family receptor 8 (IL-1R8), which also results in suppression of pro-inflammatory gene expression via inhibition of NF-kB and MAPK signaling (Li et al., 2015; Nold-Petry et al., 2015). In this study, we show that signaling through IL-1R8 is needed for inhibition of TI by IL-37.

Previous studies from our group showed that during inflammation, IL-37 restores cell energy metabolism by activating AMPK and by suppressing mTOR, both key regulator enzymes of cellular energy homeostasis (Ballak et al., 2014; Cavalli and Dinarello, 2018; Cavalli et al., 2017a; Nold et al., 2010). Here, we expand these findings by showing that IL-37 also suppresses HIF-1α and broadly counteracts the metabolic changes underlying TI. The main metabolic pathways induced by TI and reversed by treatment with IL-37 included glycolysis, glutaminolysis through the TCA cycle, purine metabolism, and tryptophan metabolism. Through this extensive metabolic reprogramming, IL-37 deprives monocytes of the energy needed to sustain chronic inflammatory activation, thus suppressing production of pro-inflammatory cytokines by "switching off" cell metabolic activation.

In humans, IL-37 primarily functions as a regulatory mechanism to limit excessive inflammation and cytokine production: accordingly, levels are abnormal in patients with inflammatory and autoimmune diseases (Cavalli and Dinarello, 2018). The inhibitory effects of IL-37 on TI observed in this study are fully consistent with suppression of pro-inflammatory cytokines and with inhibition of IL-1. The *IL37* gene is found as part of the large IL-1 gene cluster on chromosome 2q12-13, in tight proximity to the IL-1 genes: when transcription of IL-1 genes is induced by pro-inflammatory stimuli, IL-37 is simultaneously activated (Cavalli and Dinarello, 2018). Many pro-inflammatory stimuli, including cytokines or engagement of TLRs, are also recognized inducers of TI: thus, production of IL-37 likely acts as a physiologic regulatory mechanism preventing excessive or maladaptive activation of TI.

This study has some limitations. Although upregulation of the cholesterol synthesis pathway is an additional metabolic hallmark of TI (Bekkering et al., 2018), no specific lipid extraction was performed in this study for the assessment of sterol-related metabolites. Also, although TI is specific to myeloid cells (i.e., still inducible in RAG-deficient mice lacking an adaptive immune system) (Quintin et al., 2012), we cannot formally exclude that some observed inhibitory effects of IL-37 on TI may depend at least in part on modulation of adaptive immunity. Strengths of this study include the relevance of the study question, pertaining to the regulation of an emerging and pivotal immune mechanism, and the use of a broad array of relevant methodologies, in order to capture the intricacy of biological mechanisms underlying activation of TI. Despite this complexity, our findings point at one conclusion, that is, IL-37 inhibits TI.

This study has implications for the understanding of human diseases characterized by excessive activation of TI and hyper-responsiveness to inflammatory triggers, ranging from auto-inflammatory diseases (Cavalli et al., 2019; Klück et al., 2020) to severe cases of coronavirus disease 2019 (COVID-19) (Cavalli et al., 2020; Cavalli et al., 2021). Detrimental activation of TI in these conditions might be quenched by delivery of IL-37; conversely, targeted inhibition of IL-37 might boost protective TI responses during infection, vaccination, or cancer (Mulder et al., 2019; Netea et al., 2020b). Thus, determining the role of inhibitors of TI not only has critical implications for the understanding of human disease but also provides a rationale for exploring novel therapeutic strategies modulating human immunity.

STAR★METHODS

Detailed methods are provided in the online version of this paper and include the following:

- KEY RESOURCES TABLE
- RESOURCE AVAILABILITY
  - Lead contact
  - Materials availability
  - Data and code availability
- EXPERIMENTAL MODEL AND SUBJECT DETAILS
- METHOD DETAILS
  - Stimuli
  - IL-37
  - Animal studies
  - Histopathology
  - Sample processing and cell isolation
  - Neutrophil chemotaxis assays
  - Determination of soluble factors
  - ROS production assay
  - Gene expression
  - Metabolic studies
  - Extracellular Flux Analyzer (Seahorse)
  - Chromatin Immunoprecipitation
- QUANTIFICATION AND STATISTICAL ANALYSIS

SUPPLEMENTAL INFORMATION

Supplemental information can be found online at https://doi.org/10.1016/j.celrep.2021.108955.

ACKNOWLEDGMENTS

G.C. is supported by AIRC under MFAG 2018 (ID 22136 project; principal investigator [PI]); FOREUM (Career Award 2020; PI); and the Interleukin Foundation. R.J.W.A. is supported by the Netherlands Organization for Scientific Research (VENI grant 09150161810007). M.G.N. is supported by the Netherlands Organization for Scientific Research (Spinoza grant). C.A.D. is supported by the NIH (AI-15614; Charles A. Dinarello, PI).

AUTHOR CONTRIBUTIONS

G.C. and I.W.T. designed and conducted the experiments and drafted the manuscript. I.W.T., M.G., S.G., K.S., J.D.-A., R.M., D.S., E.C., and L.C. conducted the experiments. T.N., R.J.W.A., D.S., T.S.M., and A.D. conducted metabolic studies. E.Z.E. synthesized the compound. L.D., A.B., L.A.B.J., M.G.N., and C.A.D. designed the experiments, supervised the studies, and drafted the manuscript.

DECLARATION OF INTERESTS

The authors declare no competing interests.

Received: August 22, 2019
Revised: September 8, 2020
Accepted: March 17, 2021
Published: April 6, 2021

REFERENCES

Arts, R.J., Joosten, L.A., and Netea, M.G. (2016a). Immunometabolic circuits in trained immunity. Semin. Immunol. *28*, 425–430.

Arts, R.J., Novakovic, B., Ter Horst, R., Carvalho, A., Bekkering, S., Lachmandas, E., Rodrigues, F., Silvestre, R., Cheng, S.C., Wang, S.Y., et al. (2016b). Glutaminolysis and fumarate accumulation integrate immunometabolic and epigenetic programs in trained immunity. Cell Metab. *24*, 807–819.

Arts, R.J.W., Moorlag, S.J.C.F.M., Novakovic, B., Li, Y., Wang, S.Y., Oosting, M., Kumar, V., Xavier, R.J., Wijmenga, C., Joosten, L.A.B., et al. (2018). BCG vaccination protects against experimental viral infection in humans through the induction of cytokines associated with trained immunity. Cell Host Microbe *23*, 89–100.e5.

Ballak, D.B., van Diepen, J.A., Moschen, A.R., Jansen, H.J., Hijmans, A., Groenhof, G.J., Leenders, F., Bufler, P., Boekschoten, M.V., Müller, M., et al. (2014). IL-37 protects against obesity-induced inflammation and insulin resistance. Nat. Commun. *5*, 4711.

Ballak, D.B., Li, S., Cavalli, G., Stahl, J.L., Tengesdal, I.W., van Diepen, J.A., Kluck, V., Swartzwelter, B., Azam, T., Tack, C.J., et al. (2018). Interleukin-37 treatment of mice with metabolic syndrome improves insulin sensitivity and reduces pro-inflammatory cytokine production in adipose tissue. J. Biol. Chem. *293*, 14224–14236.

Bekkering, S., Quintin, J., Joosten, L.A., van der Meer, J.W., Netea, M.G., and Riksen, N.P. (2014). Oxidized low-density lipoprotein induces long-term proinflammatory cytokine production and foam cell formation via epigenetic reprogramming of monocytes. Arterioscler. Thromb. Vasc. Biol. *34*, 1731–1738.

Bekkering, S., Arts, R.J.W., Novakovic, B., Kourtzelis, I., van der Heijden, C.D.C.C., Li, Y., Popa, C.D., Ter Horst, R., van Tuijl, J., Netea-Maier, R.T., et al. (2018). Metabolic induction of trained immunity through the mevalonate pathway. Cell *172*, 135–146.e9.

Bulau, A.M., Nold, M.F., Li, S., Nold-Petry, C.A., Fink, M., Mansell, A., Schwerd, T., Hong, J., Rubartelli, A., Dinarello, C.A., and Bufler, P. (2014). Role of caspase-1 in nuclear translocation of IL-37, release of the cytokine, and IL-37 inhibition of innate immune responses. Proc. Natl. Acad. Sci. U S A *111*, 2650–2655.

Cavalli, G., and Dinarello, C.A. (2018). Suppression of inflammation and acquired immunity by IL-37. Immunol. Rev. *281*, 179–190.

Cavalli, G., Koenders, M., Kalabokis, V., Kim, J., Tan, A.C., Garlanda, C., Mantovani, A., Dagna, L., Joosten, L.A., and Dinarello, C.A. (2016). Treating experimental arthritis with the innate immune inhibitor interleukin-37 reduces joint and systemic inflammation. Rheumatology (Oxford) *55*, 2220–2229.

Cavalli, G., Justice, J.N., Boyle, K.E., D'Alessandro, A., Eisenmesser, E.Z., Herrera, J.J., Hansen, K.C., Nemkov, T., Stienstra, R., Garlanda, C., et al. (2017a). Interleukin 37 reverses the metabolic cost of inflammation, increases oxidative respiration, and improves exercise tolerance. Proc. Natl. Acad. Sci. U S A *114*, 2313–2318.

Cavalli, G., Koenders, M., Kalabokis, V., Kim, J., Choon Tan, A., Garlanda, C., Mantovani, A., Dagna, L., Joosten, L.A.B., and Dinarello, C.A. (2017b). Treating experimental arthritis with the innate immune inhibitor interleukin-37 reduces joint and systemic inflammation. Rheumatology (Oxford) *56*, 2256.

Cavalli, G., Larcher, A., Tomelleri, A., Campochiaro, C., Della-Torre, E., De Luca, G., Farina, N., Boffini, N., Ruggeri, A., Poli, A., Scarpellini, P., et al. (2021). Interleukin-1 and interleukin-6 inhibition compared with standard management in patients with COVID-19 and hyperinflammation: a cohort. The Lancet Rheumatology. https://doi.org/10.1016/S2665-9913(21)00012-6.

Cavalli, G., Tomelleri, A., De Luca, G., Campochiaro, C., Dinarello, C.A., Baldissera, E., and Dagna, L. (2019). Efficacy of canakinumab as first-line biologic agent in adult-onset Still's disease. Arthritis Res. Ther. *21*, 54.

Cavalli, G., De Luca, G., Campochiaro, C., Della-Torre, E., Ripa, M., Canetti, D., Oltolini, C., Castiglioni, B., Tassan Din, C., Boffini, N., et al. (2020). Interleukin-1 blockade with high-dose anakinra in patients with COVID-19, acute respiratory distress syndrome, and hyperinflammation: a retrospective cohort study. Lancet Rheumatol. *2*, e325–e331.

Cheng, S.C., Quintin, J., Cramer, R.A., Shepardson, K.M., Saeed, S., Kumar, V., Giamarellos-Bourboulis, E.J., Martens, J.H., Rao, N.A., Aghajanirefah, A., et al. (2014). mTOR- and HIF-1α-mediated aerobic glycolysis as metabolic basis for trained immunity. Science *345*, 1250684.

Clasquin, M.F., Melamud, E., and Rabinowitz, J.D. (2012). LC-MS data processing with MAVEN: a metabolomic analysis and visualization engine. Curr. Protoc. Bioinformatics *Chapter 14*, Unit 14.11.

Colabroy, K.L., and Begley, T.P. (2005). Tryptophan catabolism: identification and characterization of a new degradative pathway. J. Bacteriol. *187*, 7866–7869.

Czuprynski, C.J., and Brown, J.F. (1987). Recombinant murine interleukin-1 alpha enhancement of nonspecific antibacterial resistance. Infect. Immun. *55*, 2061–2065.

Dinarello, C.A., Nold-Petry, C., Nold, M., Fujita, M., Li, S., Kim, S., and Bufler, P. (2016). Suppression of innate inflammation and immunity by interleukin-37. Eur. J. Immunol. *46*, 1067–1081.

Jha, A.K., Huang, S.C., Sergushichev, A., Lampropoulou, V., Ivanova, Y., Loginicheva, E., Chmielewski, K., Stewart, K.M., Ashall, J., Everts, B., et al. (2015). Network integration of parallel metabolic and transcriptional data reveals metabolic modules that regulate macrophage polarization. Immunity *42*, 419–430.

Jung, I.D., Lee, M.G., Chang, J.H., Lee, J.S., Jeong, Y.I., Lee, C.M., Park, W.S., Han, J., Seo, S.K., Lee, S.Y., and Park, Y.M. (2009). Blockade of indoleamine 2,3-dioxygenase protects mice against lipopolysaccharide-induced endotoxin shock. J. Immunol. *182*, 3146–3154.

Kleinnijenhuis, J., Quintin, J., Preijers, F., Joosten, L.A., Jacobs, C., Xavier, R.J., van der Meer, J.W., van Crevel, R., and Netea, M.G. (2014). BCG-induced trained immunity in NK cells: role for non-specific protection to infection. Clin. Immunol. *155*, 213–219.

Klück, V., van Deuren, R.C., Cavalli, G., Shaukat, A., Arts, P., Cleophas, M.C., Crișan, T.O., Tausche, A.K., Riches, P., Dalbeth, N., et al. (2020). Rare genetic variants in interleukin-37 link this anti-inflammatory cytokine to the pathogenesis and treatment of gout. Ann. Rheum. Dis. *79*, 536–544.

Koivunen, P., Hirsilä, M., Remes, A.M., Hassinen, I.E., Kivirikko, K.I., and Myllyharju, J. (2007). Inhibition of hypoxia-inducible factor (HIF) hydroxylases by citric acid cycle intermediates: possible links between cell metabolism and stabilization of HIF. J. Biol. Chem. *282*, 4524–4532.

Li, S., Neff, C.P., Barber, K., Hong, J., Luo, Y., Azam, T., Palmer, B.E., Fujita, M., Garlanda, C., Mantovani, A., et al. (2015). Extracellular forms of IL-37 inhibit innate inflammation in vitro and in vivo but require the IL-1 family decoy receptor IL-1R8. Proc. Natl. Acad. Sci. U S A *112*, 2497–2502.

Li, S., Amo-Aparicio, J., Neff, C.P., Tengesdal, I.W., Azam, T., Palmer, B.E., López-Vales, R., Bufler, P., and Dinarello, C.A. (2019). Role for nuclear interleukin-37 in the suppression of innate immunity. Proc. Natl. Acad. Sci. U S A *116*, 4456–4461.

Lu, C., Ward, P.S., Kapoor, G.S., Rohle, D., Turcan, S., Abdel-Wahab, O., Edwards, C.R., Khanin, R., Figueroa, M.E., Melnick, A., et al. (2012). IDH mutation impairs histone demethylation and results in a block to cell differentiation. Nature *483*, 474–478.

McNamee, E.N., Masterson, J.C., Jedlicka, P., McManus, M., Grenz, A., Collins, C.B., Nold, M.F., Nold-Petry, C., Bufler, P., Dinarello, C.A., and Rivera-Nieves, J. (2011). Interleukin 37 expression protects mice from colitis. Proc. Natl. Acad. Sci. U S A *108*, 16711–16716.

Mitroulis, I., Ruppova, K., Wang, B., Chen, L.S., Grzybek, M., Grinenko, T., Eugster, A., Troullinaki, M., Palladini, A., Kourtzelis, I., et al. (2018). Modulation of myelopoiesis progenitors is an integral component of trained immunity. Cell *172*, 147–161.e12.

Moorlag, S.J.C.F.M., Röring, R.J., Joosten, L.A.B., and Netea, M.G. (2018). The role of the interleukin-1 family in trained immunity. Immunol. Rev. *281*, 28–39.

Mulder, W.J.M., Ochando, J., Joosten, L.A.B., Fayad, Z.A., and Netea, M.G. (2019). Therapeutic targeting of trained immunity. Nat. Rev. Drug Discov. *18*, 553–566.

Nemkov, T., Hansen, K.C., and D'Alessandro, A. (2017). A three-minute method for high-throughput quantitative metabolomics and quantitative tracing experiments of central carbon and nitrogen pathways. Rapid Commun. Mass Spectrom. *31*, 663–673.

Netea, M.G., Joosten, L.A., Latz, E., Mills, K.H., Natoli, G., Stunnenberg, H.G., O'Neill, L.A., and Xavier, R.J. (2016). Trained immunity: a program of innate immune memory in health and disease. Science *352*, aaf1098.

Netea, M.G., Domínguez-Andrés, J., Barreiro, L.B., Chavakis, T., Divangahi, M., Fuchs, E., Joosten, L.A.B., van der Meer, J.W.M., Mhlanga, M.M., Mulder, W.J.M., et al. (2020a). Defining trained immunity and its role in health and disease. Nat. Rev. Immunol. *20*, 375–388.

Netea, M.G., Giamarellos-Bourboulis, E.J., Domínguez-Andrés, J., Curtis, N., van Crevel, R., van de Veerdonk, F.L., and Bonten, M. (2020b). Trained immunity: a tool for reducing susceptibility to and the severity of SARS-CoV-2 infection. Cell *181*, 969–977.

Nold, M.F., Nold-Petry, C.A., Zepp, J.A., Palmer, B.E., Bufler, P., and Dinarello, C.A. (2010). IL-37 is a fundamental inhibitor of innate immunity. Nat. Immunol. *11*, 1014–1022.

Nold-Petry, C.A., Lo, C.Y., Rudloff, I., Elgass, K.D., Li, S., Gantier, M.P., Lotz-Havla, A.S., Gersting, S.W., Cho, S.X., Lao, J.C., et al. (2015). IL-37 requires the receptors IL-18Rα and IL-1R8 (SIGIRR) to carry out its multifaceted anti-inflammatory program upon innate signal transduction. Nat. Immunol. *16*, 354–365.

Pecyk, R.A., Fraser-Smith, E.B., and Matthews, T.R. (1989). Efficacy of interleukin-1 beta against systemic Candida albicans infections in normal and immunosuppressed mice. Infect. Immun. *57*, 3257–3258.

Quintin, J., Saeed, S., Martens, J.H.A., Giamarellos-Bourboulis, E.J., Ifrim, D.C., Logie, C., Jacobs, L., Jansen, T., Kullberg, B.J., Wijmenga, C., et al. (2012). Candida albicans infection affords protection against reinfection via functional reprogramming of monocytes. Cell Host Microbe *12*, 223–232.

Ross, R., Grimmel, J., Goedicke, S., Möbus, A.M., Bulau, A.M., Bufler, P., Ali, S., and Martin, M.U. (2013). Analysis of nuclear localization of interleukin-1 family cytokines by flow cytometry. J. Immunol. Methods *387*, 219–227.

Swamydas, M., Gao, J.L., Break, T.J., Johnson, M.D., Jaeger, M., Rodriguez, C.A., Lim, J.K., Green, N.M., Collar, A.L., Fischer, B.G., et al. (2016). CXCR1-mediated neutrophil degranulation and fungal killing promote Candida clearance and host survival. Sci. Transl. Med. *8*, 322ra10.

Tannahill, G.M., Curtis, A.M., Adamik, J., Palsson-McDermott, E.M., McGettrick, A.F., Goel, G., Frezza, C., Bernard, N.J., Kelly, B., Foley, N.H., et al. (2013). Succinate is an inflammatory signal that induces IL-1β through HIF-1α. Nature *496*, 238–242.

van de Veerdonk, F.L., Gresnigt, M.S., Oosting, M., van der Meer, J.W., Joosten, L.A., Netea, M.G., and Dinarello, C.A. (2015). Protective host defense against disseminated candidiasis is impaired in mice expressing human interleukin-37. Front. Microbiol. *5*, 762–802.

van der Meer, J.W.M., Barza, M., Wolff, S.M., and Dinarello, C.A. (1988). A low dose of recombinant interleukin 1 protects granulocytopenic mice from lethal gram-negative infection. Proc. Natl. Acad. Sci. USA *85*, 1620–1623.

Wirthgen, E., and Hoeflich, A. (2015). Endotoxin-induced tryptophan degradation along the kynurenine pathway: the role of indolamine 2,3-dioxygenase and aryl hydrocarbon receptor-mediated immunosuppressive effects in endotoxin tolerance and cancer and its implications for immunoparalysis. J. Amino Acids *2015*, 973548.

Xia, J., and Wishart, D.S. (2016). Using MetaboAnalyst 3.0 for comprehensive metabolomics data analysis. Curr. Protoc. Bioinformatics *55*, 14.10.1–14.10.91.

STAR★METHODS

KEY RESOURCES TABLE

REAGENT or RESOURCE	SOURCE	IDENTIFIER
Antibodies		
V450 Rat anti-CD11b	BD Biosciences	Cat# 560455
FITC Rat anti-Mouse Ly-6G	BD Biosciences	Cat# 551460
H3K4me3 Antibody - ChIP-seq Grade	Diagenode	Cat# C15410003-50
Bacterial, virus and fungal strains		
Candida albicans (Robin) Berkhout (UC820)	ATCC	ATCC® MYA-3573
Chemicals, peptides, and recombinant proteins		
Glucan from baker's yeast (S. cerevisiae)	Sigma-Aldrich	Cat# G5011-25MG
Lipopolysaccharide (LPS)	Sigma-Aldrich	Cat# L9641
Recombinant IL-37 isoform b (residues 46–218)	Prof. Dinarello C.A.	N/A
Phosphate Buffered Saline (PBS)	Corning®	Cat# 21-040-CV
RPMI 1640, 1X	Corning®	Cat# 10-040-CV
Penicillin-Streptomycin Solution, 100x	Corning®	Cat# 30-002-CI
SuperScript III First-Strand Synthesis System	ThermoFisher Scientific	Cat# 18080051
Power SYBR Green Master Mi	ThermoFisher Scientific	Cat# 4368577
Corning® Cell-Tak Cell Tissue Adhesive	Sigma_Aldrich	Cat# DLW354242
Agilent Seahorse XF DMEM Medium pH 7.4	Agilent	Cat# 103575-100
Critical commercial assays		
Neutrophil Isolation Kit, mouse	Miltenyi Biotec	Cat# 130-097-658
Mouse CXCL1/KC DuoSet ELISA	BioTechne	Cat# DY453
Mouse Myeloperoxidase DuoSet ELISA	BioTechne	Cat# DY3667
Mouse IL-1 beta/IL-1F2 DuoSet ELISA	BioTechne	Cat# DY401
Mouse IL-6 DuoSet ELISA	BioTechne	Cat# DY406
Mouse TNF-alpha DuoSet ELISA ouseT TNFalphaDuoSet ELISA	BioTechne	Cat# DY410
L-Lactate Assay Kit (Colorimetric)	abcam	Cat# ab65331
Cellular ROS Assay Kit (Deep Red)	abcam	Cat# ab186029
Seahorse XF Glycolysis Stress Test Kit	Agilent	Cat# 103020-100
MinElute PCR Purification Kit	QIAGEN	Cat# 28004
Experimental models: Organisms/strains		
Male C57BL/6J mice aged 10-12 weeks	The Jackson Laboratories	Cat# 000664 | B6
Male IL-1R8 deficient (−/−)	kind gift from Dr. Mayumi Fujita.	N/A
Oligonucleotides		
Forward Primer for *Hk1* mRNA: 5′-TGCCATGCGGCTCTCTGATG-3′	This paper	N/A
Reverse Primer for *Hk1* mRNA: 5′-CTTGACGGAGGCCGTTGGGTT-3′	This paper	N/A
Forward Primer for *Pk* mRNA: 5′-CCCATCACGGCCCGCAACACT-3′	This paper	N/A
Reverse Primer for *Pk* mRNA: 5′-ATTCAGCCGAGCCACATTCATTCC-3′	This paper	N/A
Forward Primer for *Hif1a* mRNA: 5′-CTATGGAGGCCAGAAGAGGGTAT-3′	This paper	N/A

(*Continued on next page*)

Continued

REAGENT or RESOURCE	SOURCE	IDENTIFIER
Reverse Primer for *Hif1a* mRNA: 5′-CCCACATCAGGTGGCTCATAA-3′	This paper	N/A
Forward Primer for *Il6* mRNA: 5′-TGCACAAAATTTGGAGGTGA-3′	This paper	N/A
Reverse Primer for *Il6* mRNA: 5′-ACCCAACCTGGACAACAGAC-3′	This paper	N/A
Forward Primer for *Tnfa* mRNA: 5′-CTTGGGCCAGTGAGTGAAAG-3′,	This paper	N/A
Reverse Primer for *Tnfa* mRNA: 5′-TAGCCAGGAGGGAGAACAGA-3′	This paper	N/A
Software and algorithms		
BD FACS Diva software	BD Biosciences	N/A
MetaboAnalyst package	Xia and Wishart, 2016	https://www.metaboanalyst.ca
GraphPad Prism	GraphPad Software Inc	https://www.graphpad.com
GENE E software	Broad Institute	N/A

RESOURCE AVAILABILITY

Lead contact

Further information and requests for resources and reagents should be directed to and will be fulfilled by Prof. Charles Dinarello (cdinare333@aol.com).

Materials availability

This study did not generate new unique reagents.

Data and code availability

This study did not generate any unique datasets or code.

EXPERIMENTAL MODEL AND SUBJECT DETAILS

Male C57BL/6J mice aged 10-12 weeks were purchased from Jackson Laboratories (Bar Harbor, Maine, USA) and housed under standard conditions. The weight range for all animals used in the experiments was between 21 and 24 g. Male IL-1R8 deficient (−/−) mice were a kind gift from Dr. Mayumi Fujita. Animal studies followed the NIH Guidelines for the Care and Use of Laboratory Animals, as well as protocols approved by the Institutional Animal Care and Use Committees of the University of Colorado Denver, Aurora, CO, USA and of IRCCS San Raffaele Institute, Milan, Italy.

METHOD DETAILS

Stimuli

The *Candida albicans* strain ATCC MYA-3573 (UC 820) was used in all experiments. *C. albicans* was grown overnight in Sabouraud broth at 37°C; cells were harvested by centrifugation, washed twice in sterile PBS and suspended to a concentration of 10×10^6/mL prior to inoculum. β-glucan and lipopolysaccharide (LPS) were purchased from Sigma-Aldrich (St. Louis, MO). Sterile PBS (Corning, Tewksbury, MA) was used as vehicle.

IL-37

IL-37 is transcribed as five different splice variants (IL-37a–e), with IL-37b being the most complete and best-characterized isoform (Cavalli and Dinarello, 2018; Dinarello et al., 2016). IL-37b with an N terminus at valine 46 and C terminus at 218 (46-218) was generated as previously reported (Cavalli et al., 2017a). Briefly, IL-37 residues 46-218 was cloned into a pET21 vector with an N-terminal 6xHis tag and thrombin cleavage site. Protein was expressed in BL21/DE3 cells at 37°C and purified via Ni affinity chromatography. Eluted fractions containing IL-37 were dialyzed into 50mM tris, pH 7.2, 100mM NaCl, 1mM EDTA and applied onto an SP ion exchange using SP fast-flow resin (GE Healthcare). SP ion exchange eluted fractions were concentrated and cleaved with thrombin to remove the 6xHis tag for a final application to size-exclusion chromatography in PBS using a Superdex-75 (GE Healthcare).

Animal studies

To induce trained immunity *in vivo* in mice, a single dose of β-glucan 1 mg in 200 μL PBS was administered intraperitoneally 3 days before infection (day −3), as previously reported (Mitroulis et al., 2018). Recombinant human IL-37 1μg/mouse in 200 μL PBS was administered intraperitoneally on day −3 (2 h prior to administration of β-glucan), day −2, and day −1. On day 0, mice were injected intravenously with *C. albicans* yeast (2×10^6 CFU/mouse suspended in 100 μL PBS). Survival and changes in body weight were assessed daily for 2 weeks. In a separate experiment, animals were sacrificed on day 4 after infection to assess the tissue fungal burden: kidneys were aseptically removed, weighted, and homogenized in sterile PBS using a tissue grinder. The number of *C. albicans* cells in the tissues was then determined by plating serial dilutions on Sabouraud dextrose agar plates. The number of CFU was assessed after 24 h of incubation at 37°C, and expressed as log CFU/g tissue.

Histopathology

Kidneys were harvested for histological examination at day 4 after infection. The tissues were fixed in formalin and embedded in paraffin. Tissue sections (5 μm) were stained with Hematoxylin & Eosin (H&E) to study cell influx. Pictures were obtained from histology slides using a Zeiss microscope fitted with an Axiocam camera.

Sample processing and cell isolation

Mice were anesthetized and whole blood was obtained by orbital bleeding into heparinized tubes prior to sacrifice. Bone marrow cells were collected from both femurs through flushing with ice-cold RPMI, passed through a 70-μm cell strainer, washed, and suspended in RPMI (Corning) supplemented with 1% penicillin/streptomycin at $5x10^6$ cell/ml. Cells were seeded at $0.5x10^6$/well in 96-flat bottom well plates in 200 μl RPMI, and incubated for 2 h at 37°C in 5% CO_2; adherent monocytes were isolated by removing non-adherent cells with warm RPMI.

Neutrophil chemotaxis assays

Neutrophils were isolated from the bone marrow of healthy, unchallenged mice using the Neutrophil isolation kit (Miltenyi), incubated with fluorescently labeled antibodies against mouse CD11b V450, and Ly6g FITC (BD Bioscience) or corresponding isotype controls, and fixed with 2% paraformaldehyde. Neutrophil sorting and assessment of purity (> 95%) and count were performed by flow cytometry using BD FACSCanto II (BD Biosciences). Data was analyzed using BD FACS Diva software (BD Biosciences). Neutrophil chemotaxis was evaluated with a migration (or 'Boyden chamber') assay: the kidney homogenate solution was placed into the lower chamber, while cells (1×10^6) were placed into the upper chamber, separated by a transwell 5.0 μm pore permeable membrane (Corning). After incubation for 3 h at 37°C and 5% CO_2, counting cells in both chambers allowed quantification of migration, expressed as 'migration index' (ratio of cells in the lower to top chamber).

Determination of soluble factors

Levels of mouse KC, MPO, IL-1β, IL-6, and TNFα in kidney homogenates were determined with appropriate ELISA kits (BioTechne, Minneapolis, MN). Lactate was measured with a Colorimetric Assay Kit (Abcam, Cambridge, MA).

ROS production assay

β-glucan and IL-37 were administered *in vivo* and monocytes were collected as described above and seeded overnight in a 96-well plate at a concentration of 2.5×10^4 cells per well. ROS production was determined using a Cellular ROS Assay Kit per manufacturer's recommendations (Abcam, Cambridge, MA). Relative ROS quantitation was determined as percent of change from control after background subtraction.

Gene expression

β-glucan and IL-37 were administered *in vivo* and monocyte collection were performed as described above. RNA was then isolated using Trizol (Thermo Fisher Scientific) and synthesized in cDNA using SuperScript III First-Strand (Thermo Fisher Scientific). Quantitative PCR (qPCR) was performed on cDNA using Power SYBR Green PCR master mix (Thermo Fisher Scientific) on Biorad CFX96 Real time system. Gene expression was assessed for the following mRNAs: *Hk1* (forward 5′TGCCATGCGGCTCTCTGATG-3′ and reverse, 5′- CTTGACGGAGGCCGTTGGGTT-3′), *Pk* (forward 5′ - CCCATCACGGCCCGCAACACT −3′ and reverse5′ATTCAGC CGAGCCACATTCATTCC-3′) and *Hif1a* (forward 5′-CTATGGAGGCCAGAAGAGGGTAT-3′ 5′-CCCACATCAGGTGGCTCATAA-3′) with *gapdh* used as a reference gene.

Metabolic studies

Monocytes from mice treated with β-glucan and IL-37 *in vivo* were lysed in 100 μl of ice-cold extraction buffer (methanol: acetonitrile: water 5:3:2), vortexed for 30 min at 4°C, and centrifuged at 15000 g for 10 minutes at 4°C. After discarding protein pellets, 20 μl of the supernatant fractions were assayed as previously described with additional adjustments (Nemkov et al., 2017). Briefly, the analytical platform employs a Vanquish UHPLC system (Thermo Fisher Scientific, San Jose, CA, USA) coupled online to a Q Exactive mass spectrometer (Thermo Fisher Scientific, San Jose, CA, USA). Samples were resolved over a Kinetex C18 column, 2.1 × 150 mm, 1.7 μm particle size (Phenomenex, Torrance, CA, USA) equipped with a guard column (SecurityGuard™ Ultracartridge – UHPLC

C18 for 2.1 mm ID Columns – AJO-8782 – Phenomenex, Torrance, CA, USA) using an aqueous phase (A) of water and 0.1% formic acid and a mobile phase (B) of acetonitrile and 0.1% formic acid for positive ion polarity mode, and an aqueous phase (A) of water: acetonitrile (95:5) with 1 mM ammonium acetate and a mobile phase (B) of acetonitrile:water (95:5) with 1 mM ammonium acetate for negative ion polarity mode. Samples were eluted from the column using either an isocratic elution of 5% B flowed at 250 μl/min and 25°C or a gradient from 5% to 95% B over 1 minute, followed by an isocratic hold at 95% B for 2 minutes, flowed at 400 μl/min and 30°C. The Q Exactive mass spectrometer (Thermo Fisher Scientific, San Jose, CA, USA) was operated independently in positive or negative ion mode, scanning in Full MS mode (2 μscans) from 60 to 900 m/z at 70,000 resolution, with 4 kV spray voltage, 15 sheath gas, 5 auxiliary gas. Calibration was performed prior to analysis using the Pierce™ Positive and Negative Ion Calibration Solutions (Thermo Fisher Scientific). Acquired data was then converted from .raw to .mzXML file format using Mass Matrix (Cleveland, OH, USA). Metabolite assignments, isotopologue distributions, and correction for expected natural abundances of deuterium, ^{13}C, and ^{15}N isotopes were performed using MAVEN (Princeton, NJ, USA) (Clasquin et al., 2012). Graphs, heatmaps and statistical analyses (either T-Test or ANOVA), metabolic pathway analysis, PLS-DA and hierarchical clustering was performed using the MetaboAnalyst package (https://www.metaboanalyst.ca) (Xia and Wishart, 2016).

Extracellular Flux Analyzer (Seahorse)

Bone marrow-derived monocytes were treated with IL-37 (10ng/ml) for 2 hours prior to stimulation with β-glucan (200ng/mL) or vehicle for 12 hours. Five days later, OCR and ECAR were measured by Seahorse XFe96 Analyzer (Agilent Technologies, Santa Clara, CA, USA) using SeaHorse XF96 Glycolysis Stress Test, following the manufacturer's instructions. Briefly, the day of the assay cells were counted and attached to 96-well Seahorse cell culture microplates, pre-coated with Corning Cell-Tak (Life Sciences) according to manufacturer's instructions, at a density of 70,000 cells per well, in Seahorse XF Base Medium pH 7.4 with 1 mM HEPES (Agilent Technologies). The medium was supplemented with 2 mM L-glutamine for Glycolysis Stress Test assay. The plate was incubated at 37 °C for 1 h in a non-CO2 incubator. OCR was assessed at baseline. For the Glycolysis Stress Test assay after ECAR baseline measurements, glucose, oligomycin A, and 2-deoxy-glucose (2-DG) were added sequentially to each well to reach the final concentrations of 10 mM, 2 μM, and 50 mM, respectively. Glycolysis was calculated by subtracting the last ECAR measurement before glucose injection from the maximum ECAR measurement before oligomycin injection; the glycolytic capacity was calculated by subtracting the last ECAR measurement before glucose injection from the maximum ECAR measurement before 2-DG injection. OCR data are expressed as pmol of oxygen per minute per arbitrary units (pmol/min), ECAR data as mpH per minute per arbitrary units (mpH/min).

Chromatin Immunoprecipitation

Purified cells were fixed with 1% formaldehyde (Sigma) at a concentration of approximately 10^6 cells/mL. Fixed cell preparations were sonicated using a Diagenode Bioruptor UCD-300 for 3 × 10 min (30 s on; 30 s off). 33 μL of chromatin (one million cells) were incubated with 255 μL dilution buffer, 12 μL protease inhibitor cocktail and 0.5−1 μL of H3K4me3 antibody (Diagenode) and incubated overnight at 4°C with rotation. Protein A/G magnetic beads were washed in dilution buffer with 0.15% SDS and 0.1% BSA, added to the chromatin/antibody mix and rotated for 60 min at 4°C. Beads were washed with 500 μL buffer for 5 min at 4°C with five rounds of washes. After washing chromatin was eluted using elution buffer for 20 min. Supernatant was collected, 8 μL 5M NaCl, 2 μL proteinase K were added and samples were incubated for 4 h at 65°C. Finally, samples were purified using QIAGEN; Qiaquick MinElute PCR purification Kit and eluted in 20 mL EB. Primer pairs employed for quantitative PCR were as follows:

Il6 forward: TGCACAAAATTTGGAGGTGA; *Il6* reverse: ACCCAACCTGGACAACAGAC. *Tnfa* forward: CTTGGGCCAGTGAGTGAAAG; *Tnfa* reverse: TAGCCAGGAGGGAGAACAGA.

QUANTIFICATION AND STATISTICAL ANALYSIS

Significance of differences was evaluated with Mann-Whitney or ANOVA test using GraphPad Prism (GraphPad Software Inc, La Jolla, CA). Differences in survival experiments were calculated using the product limit method of Kaplan and Meier. Hierarchical clustering analysis for metabolic studies was performed with GENE E software (Broad Institute). Detailed information on each experiment is provided in the respective Figure Legends. Statistical significance was set at $p < 0.05$.